Electronic Supplementary Material (ESI) for Energy & Environmental Science.

Supporting Information

This PDF file includes:

Supporting Notes 1-6

Supporting Figures 1-13

1. Supporting Notes

Supporting Note 1 | Exfoliation of Ti_3AlC_2 powders

First, 0.66g lithium fluoride (LiF) is added into 10 mL 9 M HCl solution with stirring at room temperature to dissolve the salt powder. Then 1.5 g Ti_3AlC_2 powders are gradually immersed in the mixture solution to avoid violent exothermic reaction and the resulting mixture solution is reacting at 35°C for 24 h. Obtained deposition is washed *via* deionized water until pH~7, and dried in air for 12 hours. The multilayer $Ti_3C_2T_x$ could be obtained.

Supporting Note 2 | Delamination of $Ti_3C_2T_x$ and the preparation of MXene/CNF composite membranes

To delaminate $Ti_3C_2T_x$, the solution is dissolved into DMSO and magnetically stirred at room temperature and then centrifuged and cleaned with deionized (DI) water. The resulting $Ti_3C_2T_x$ solution is dispersed in DI water with a concentration of 1 mg/mL, following 10-minutes sonication under flowing argon, and then centrifugation for 1 h at 3500 r.p.m. The supernatant including stable few-layered $Ti_3C_2T_x$ nanosheets is collected. Then a certain amount of dispersed $Ti_3C_2T_x$ nanosheets and CNFs could be assembled into a nanofluidic membrane upon vacuum filtration on a polycarbonate (PC, an average pore size of 200 nm), and membranes can be exfoliated from substrates after drying.

Supporting Note 3 | Electrical measurements

The ionic transport properties and subsequent energy conversion tests of MXene membranes were performed with a Keithley 6487 semiconductor picoammeter (Keithley Instruments, Cleveland, OH). The membranes were mounted between a two-compartment conductivity cell. Ag/AgCl electrodes are used during the entire testing process. All measurements are carried out at room temperature.

Supporting Note 4 | Supporting electrolyte

Considering the solubility product (K_{sp}) of the AgCl and AgOH (easily converted to Ag_2O). The K_{sp} (298.15 K) of AgCl and AgOH (Ag_2O) are 1.77×10^{-10} and 2.0×10^{-8} (*CRC Handbook of chemistry and physical*), respectively.

When $[Ag^+][OH^-] > K_{sp}$ (AgOH), AgOH would form.

When $[Ag^+][Cl^-] > K_{sp}$ (AgCl), AgCl would form.

In order to form AgCl in the precipitation process and keep AgOH (Ag_2O) in a soluble state, the following conditions need to be satisfied:

$$[\mathrm{Cl}^-] > \frac{K_{sp}\,(AgCl)}{K_{sp}\,(AgOH)/[OH^-]} \qquad \text{(S1)}$$

In the manuscript, the maximum concentration of NaOH is 0.01 M, and the concentration of Cl^- needs to be above 8.85×10^{-5} M to avoid the form of AgOH(Ag_2O). Therefore, 10^{-4} M NaCl is selected as the supporting electrolyte.

Supporting Note 5 | Calculation of the layer spacing

The (002) peak in XRD shows a strong and single peak at 6.97°. According to Bragg's law:

$$2d\sin\theta = n\lambda \qquad \text{(S2)}$$

d is the layer spacing; θ is the angle between the incident wave and the scattering plane, λ is the wavelength of the incident wave and n = 1. Here, 2θ (002)=6.11° and the corresponding d (002) = 1.44 nm. So, the highly uniform lamellar structure of the membrane is with a layer spacing of 0.44 nm considering of the thickness of single-layer $Ti_3C_2T_x$ nanosheet.

Supporting Note 6 | Numerical simulation

The thermoelectric conversion phenomenon was theoretically investigated using commercial finite-element software package COMSOL (version 5.4) Multiphysic based on "electrostatics (Poisson equation)" and "Nernst-Planck without Electroneutrality" modules. The coupled governing Poisson and Nernst-Planck (PNP) Equations are shown as below:

$$J_i = D_i\left(\nabla c_i + \frac{z_i F c_i}{RT}\nabla\varphi\right) + c_i u \qquad \text{(S3)}$$

$$\nabla^2\varphi = -\frac{F}{\varepsilon}\sum z_i c_i \qquad \text{(S4)}$$

$$\nabla\cdot J_i = 0 \qquad \text{(S5)}$$

Here, the physical quantities J_i, D_i, c_i, φ, u, R, F, T, and ε refer to the ionic flux, diffusion coefficient, ion concentration, electrical potential, fluid velocity, universal gas constant, Faraday constant, absolute temperature, and dielectric constant of the electrolyte solutions, respectively. The equation (S3) is the Nernst–Planck equation which describes the transport property of a charged nanochannel. Equation (S4) is the Poisson equation which describes the relationship between the electrical potential and ion concentrations. Besides, the flux should satisfy the time-independent continuity equation (S5) when the system reaches a stationary regime. A simplified negative-charged (σ_{surface} = -0.02 mC/m^2 and σ_{space}=-8 C/cm^3) channel with a length of 1000 nm, a width of 500 nm, and a height of 0.44 nm was chosen as the simulated model (Figure S10) and the concentration of the electrolyte in the two reservoirs is set to 50-fold (i.e. 0.5 M/0.01 M). To carry out the calculations, the “Electrostatics (AD/DC Module)” and “Nernst-Plank without Electroneutrality” modules are used. Besides, to precisely setup the temperature of the channel, the “Heat Transfer in Fluids” module was coupled to this model. The chemical reaction rate of acid-base neutralization is determined by the Arrhenius equation, hydrogen ion concentration, and hydroxide ion concentration:

$$K = A\frac{-E_a}{RT} \tag{S6}$$

K represents chemical rate constant, R is gas constant, T is the absolute temperature, E_{a} represents apparent activation energy, A represents pre-exponential factor.

The coupled Equation (S3) to (S6) must be solved for given geometry using appropriate boundary conditions.

The boundary condition for the potential φ on the channel wall is

$$\underset{n}{\rightarrow} \cdot \nabla\varphi =-\frac{\sigma}{\varepsilon} \tag{S7}$$

The ion flux has the zero normal components at the boundaries:

$$\underset{n}{\rightarrow} \cdot J = 0 \tag{S8}$$

The parameter σ (σ is set to -0.025 mC/m^2) is the surface charge density of the channel walls. Then, the ionic current can be calculated by:

$$I = \int_s F(z_p j_p + z_n j_n) \cdot \underset{n}{\rightarrow} dS \tag{S9}$$

2. Supporting Figures

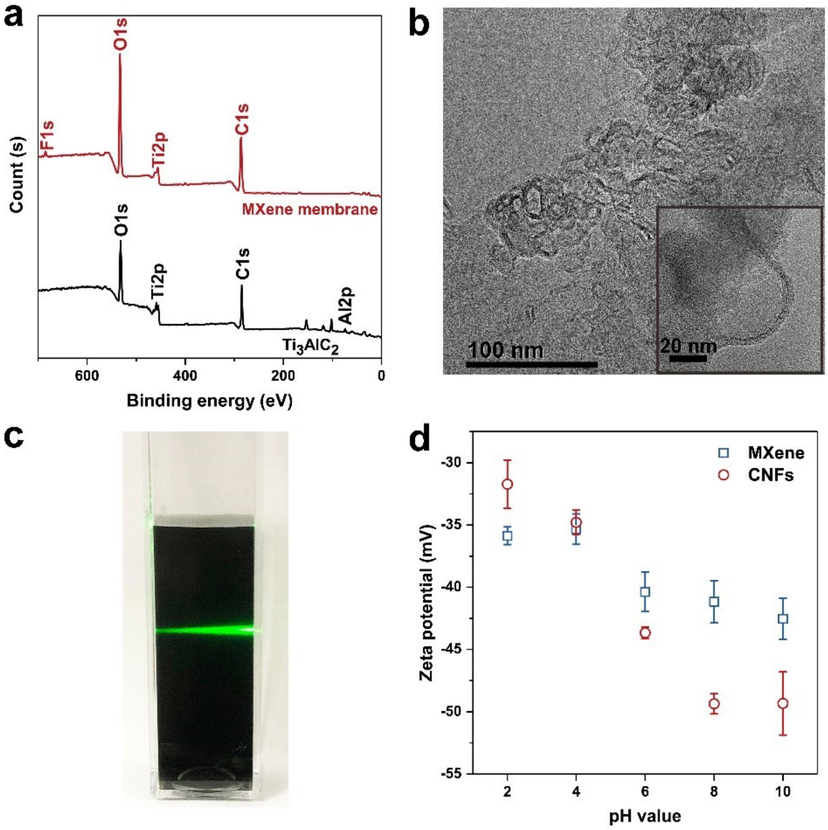

Figure S1 (a) X-ray photoelectron spectroscopy (XPS) scans of Ti_3AlC_2 and MXene. The disappearance of the aluminum peak and the appearance of fluorine and hydrogen indicate the successful etching and the emerging of hydroxide and fluoride surface groups on the $Ti_3C_2T_x$ nanosheets. (b) TEM image of the CNF (Inside shows a single cellulose nanofiber with a diameter of a few nanometers). (c) The Tyndall scattering effect of the as-prepared $Ti_3C_2T_x$/CNF colloidal suspension, indicating the good dispersion in water. (d) Zeta potential of the MXene and CNF at various pH values, suggesting that they are both negatively charged in the whole pH range from 2 to 10.

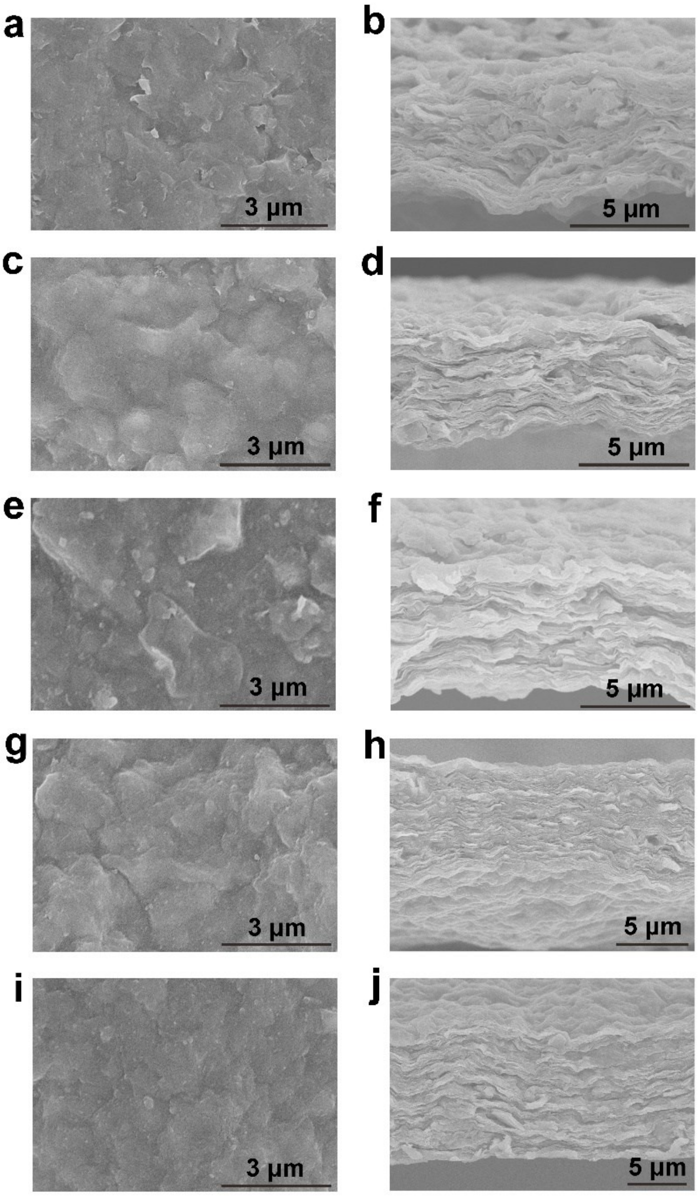

Figure S2 Surface and cross-sectional SEM images of MXene/CNF composite membrane with different CNF weight percentages. (a-b) 0%; (c-d) 5%; (e-f) 10%; (g-h) 15%; (i-j) 20%.

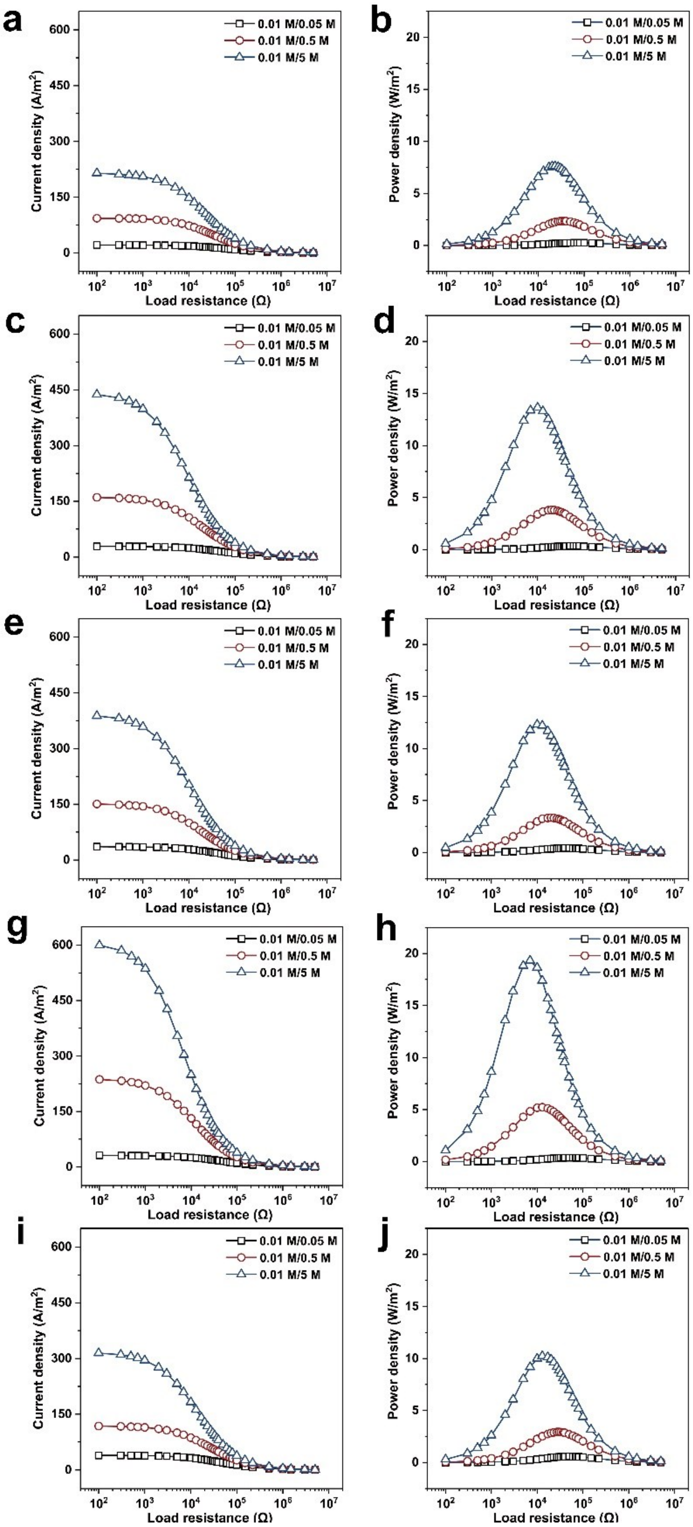

Figure S3 Current density and power density of MXene/CNF composite membrane with different CNF weight percentages. (a-b) 0%; (c-d) 5%; (e-f) 15%; (g-h) 15%; (i-j) 20%.

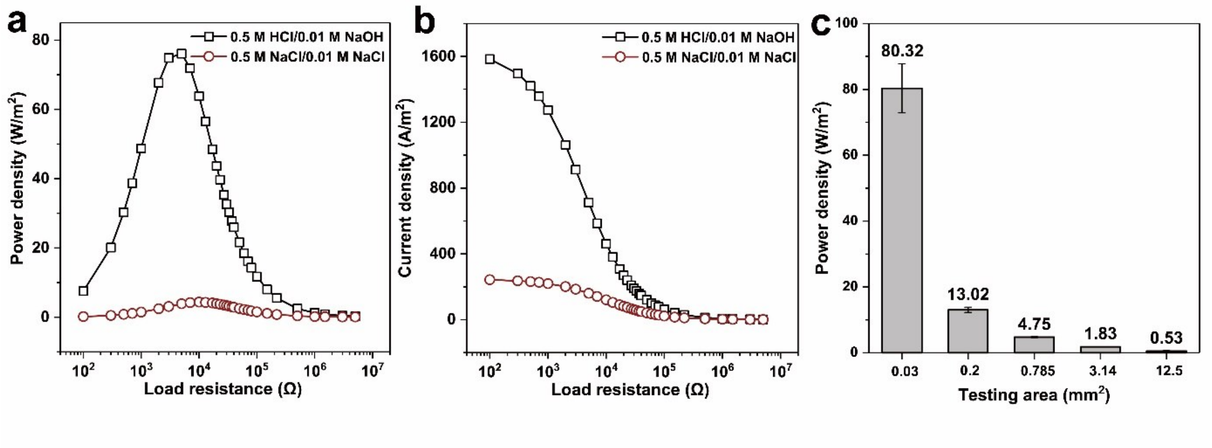

Figure S4 (a) The power density and (b) current density as a function of resistance under 50-fold concentration gradient before and after the assistance of chemical reaction. (c) Power density of chemical reaction enhanced energy conversion system under a series of testing areas.

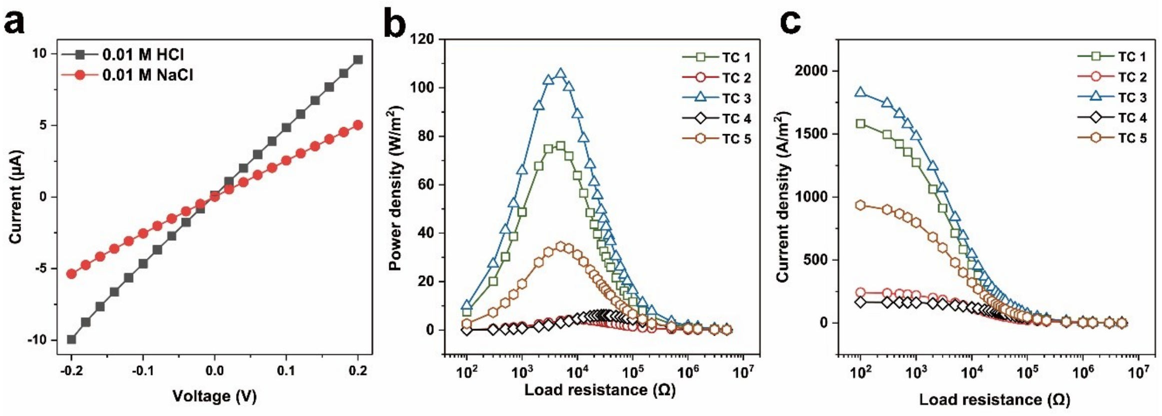

Figure S5 (a) The I-V curves of the membrane in 0.01 M NaCl and 0.01 HCl solutions, respectively. (b-c) Power generation of a composite membrane with a CNF weight percentage of 10% under five test conditions. TC 1: 0.5 M HCl/0.01 M NaOH; TC 2: 0.5 M NaCl/0.01 M NaCl; TC 3: 0.49 M HCl+0.01 M NaCl/0.01 M NaOH; TC 4: 0.01 M HCl/0.01 M NaOH; TC 5: 0.5 M HCl/0.01 M HCl.

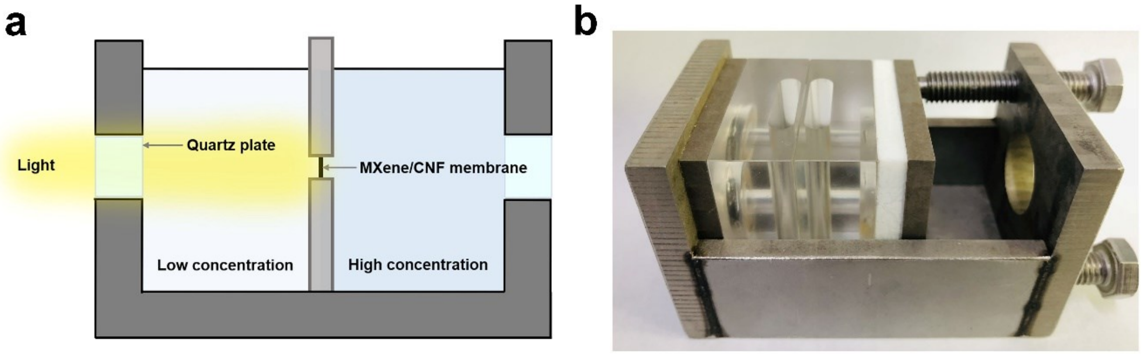

Figure S6 (a) Scheme and (b) photograph of the measuring device.

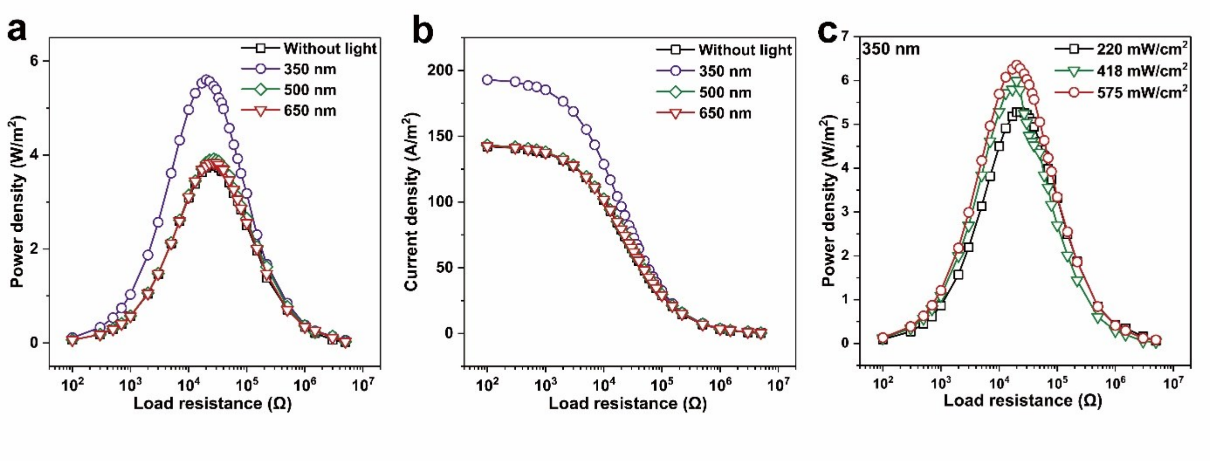

Figure S7 (a) The power density and (b) current density of a composite membrane with a CNF weight percentage of 10% without light and under irradiation with different wavelength under 50-fold salinity gradient (0.5 M NaCl/0.01 M NaCl). (c) Power density of a composite membrane with a CNF weight percentage of 10% under irradiation with different intensity (350 nm).

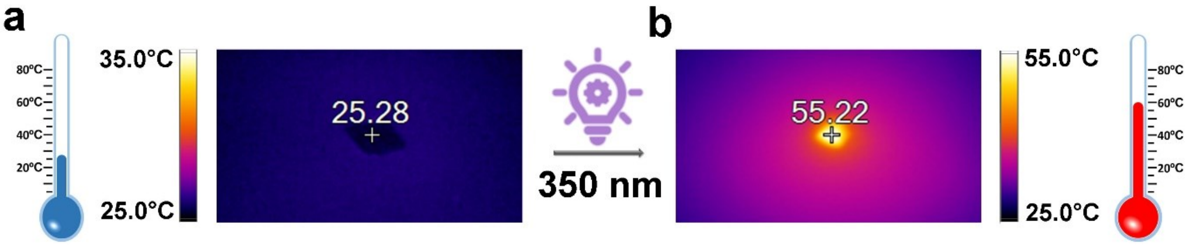

Figure S8 IR camera images a MXene/CNF composite membrane with a CNF weight percentage of 10% before and after 350 nm light illumination.

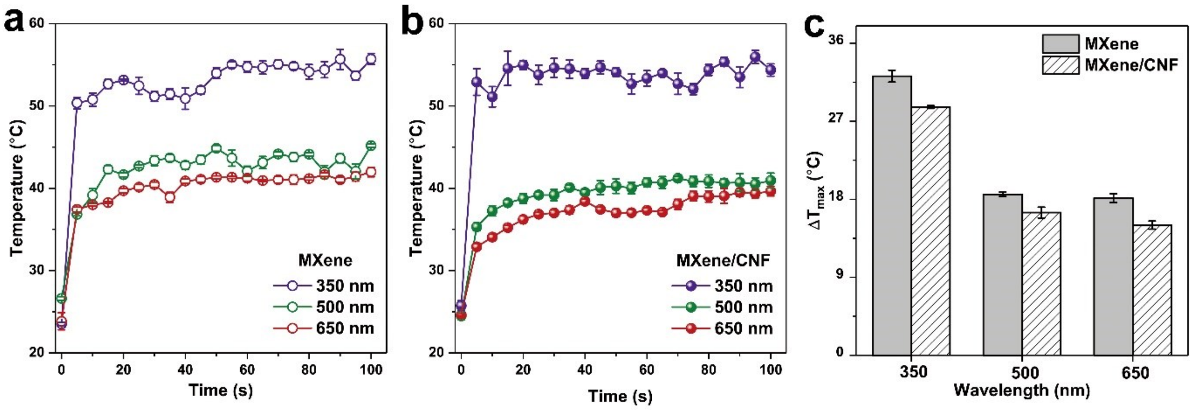

Figure S9 Photothermal performance of MXene membrane and MXene/CNF composite membrane under irradiation with different wavelength (~220 mW/cm^2).

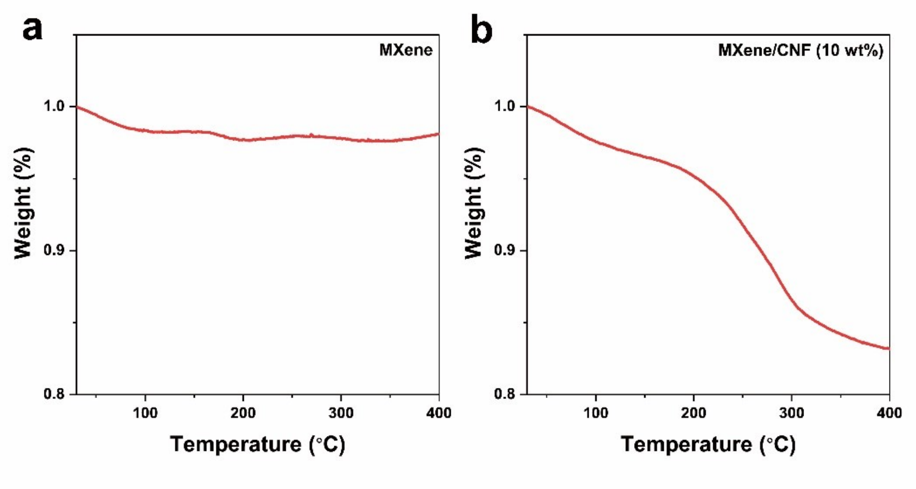

Figure S10 Thermogravimetric analysis from 30 to 400°C of (a) the MXene membrane and (a) MXene/CNF composite membrane. At temperatures above 250°C, cellulose is entirely decomposed due to the breaking down of its molecular structure, thus resulting in a gradual weight loss when the composite membrane was heated to 400°C.

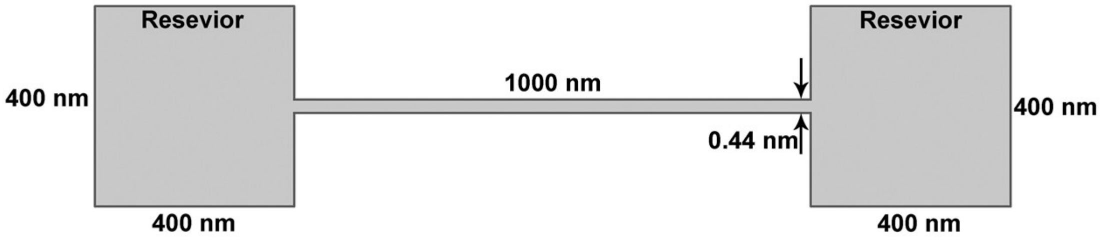

Figure S11 Model of theoretical simulation. (Drawing not to scale.)

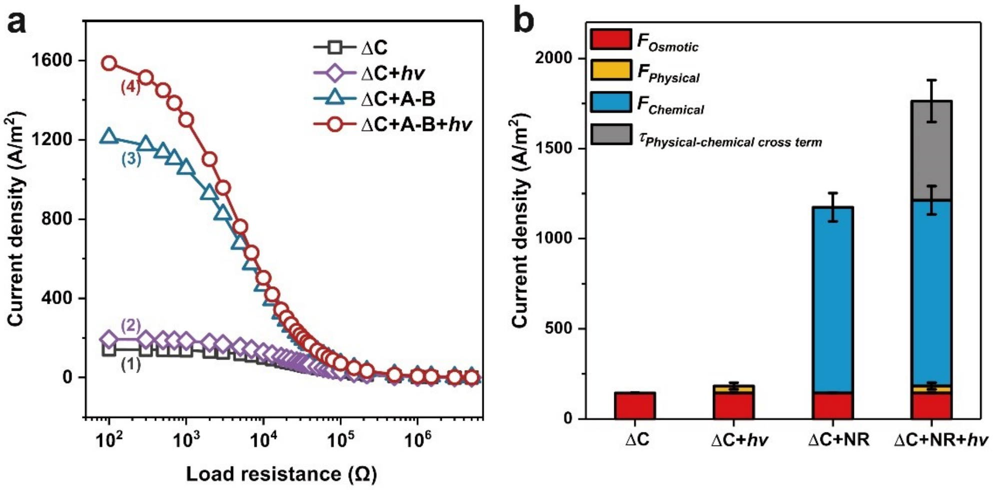

Figure S12 (a) Recorded current density of the four models as a function of the load resistance in experiment [ΔC: under concentration gradient; *hv*: under irradiation with 350 nm light (light intensity ~260 mW·cm^{-2}); A-B: introduction of acid-base reaction (0.5 M HCl/0.01 M NaOH)]. (b) The corresponding current density under four conditions (Different colors refer to the contribution of different factors to the power density).

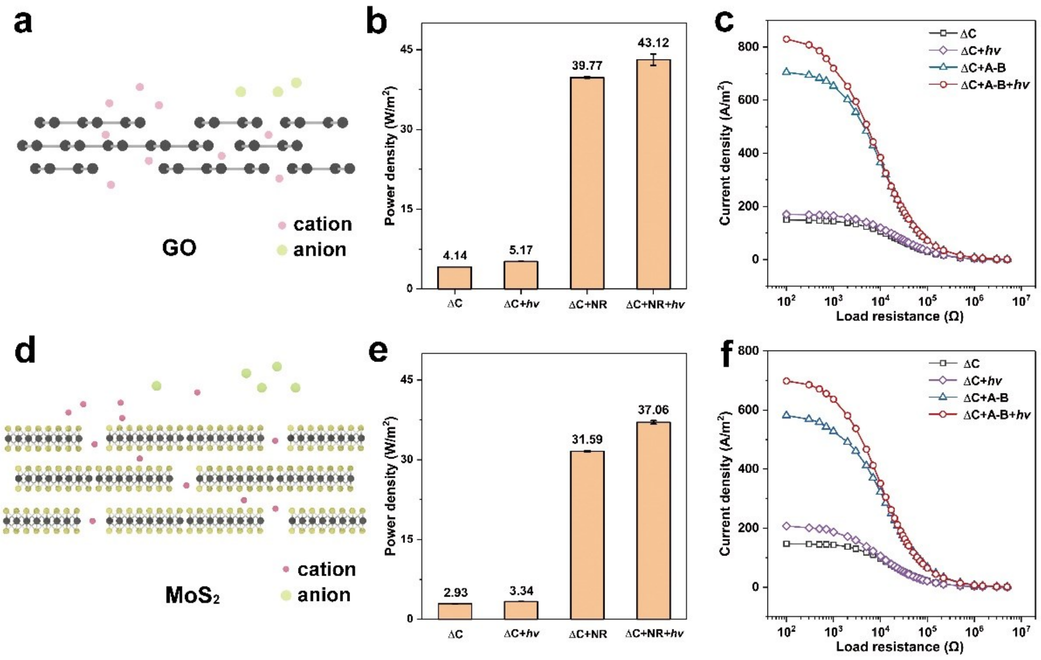

Figure S13 Physical-chemical hybrid factors enhanced osmotic energy conversion system through (a-c) 2D GO membrane and (b-d) MoS_2 membrane. For the 2D GO membrane, the power density reached a maximum value of ~4.14 W/m^2 when there is only a concentration difference (ΔC, 0.5 M NaCl, and 0.01 M NaCl). After the introduction of light (ΔC+*hv*) to the low-concentration side, the power density increased to 5.17 W/m^2. In addition, the output power density reached a maximum value of ~39.77 W/m^2 with 0.5 M HCl and 0.01 M NaOH (ΔC+A-B), which is much higher than that using NaCl at the same concentration gradient (ΔC=50-fold). By introducing both light and chemical reaction (ΔC+A-B+*hv*), the power density could be improved to ~43.12 W/m^2. For the MoS_2-based 2D nanofluidic system, the output power density reached a maximum value of ~2.93 W/m^2, 3.34 W/m^2, 31.59 W/m^2, and 37.06 W/m^2 under the four conditions.